# Degradation Kinetics of Model Hyperbranched Chains with Uniform Subchains and Controlled Locations of Cleavable Disulfide Linkages

Lianwei Li,*[,†] Xu Wang,[†] Jinxian Yang,[†] Xiaodong Ye,*[,†] and Chi Wu[†,‡]

[†]Hefei National Laboratory for Physical Sciences at the Microscale, Department of Chemical Physics, University of Science and Technology of China, Hefei, Anhui 230026, China

[‡]Department of Chemistry, The Chinese University of Hong Kong, Shatin N. T., Hong Kong

ABSTRACT: We developed a strategy to make model hyperbranched structure with uniform subchains and controlled locations of cleavable linkages. First, a novel seesaw-type tetrafunctional initiator with one alkyne, one disulfide linkage, and two bromine groups ($\equiv-S-S-(Br)_2$) was prepared. Using such an initiator, an AB_2-type macromonomer (azide~~alkyne~~azide) with one disulfide linkage at its center was prepared via successive atom transfer radical polymerization (ATRP) and azidation substitution reaction, where ~~ represents polystyrene chains. Further interchain "clicking" coupling between the azide and alkyne groups on the macromonomers led to model hyperbranched polystyrenes with uniform subchains and controllablly located cleavable disulfide linkages. The ^{1}H nuclear magnetic resonance spectra, Fourier transform infrared spectroscopy, and size exclusion chromatography with a multiangle laser light scattering detector confirmed the designed degradable hyperbranched structure. Armed with this novel sample, we studied its dithiothreitol (DTT)-induced degradation in various organic solvents by a combination of static and dynamic LLS. We found that the cleavage of disulfide bonds contains a fast and a slow process. The fast one reflects the degradation of disulfide bonds on the chain periphery; while the slow one involves those inside. Both the fast and slow degradation reaction rate constants (K_{fast} and K_{slow}) are a linear function of the initial DTT concentration ($[DTT]_0$), but the relative contribution of the two processes is mainly governed by the hyperbranched chain structure, nearly independent of $[DTT]_0$.
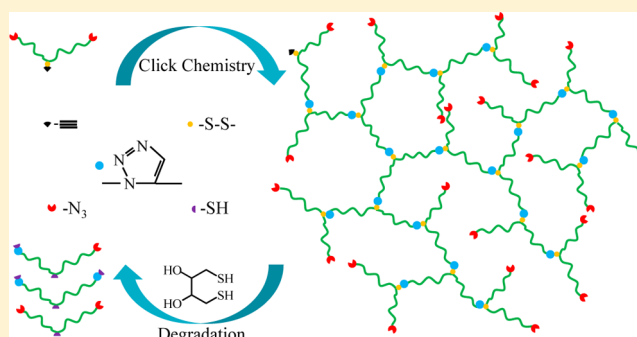
INTRODUCTION

In the past two decades, various nonideal hyperbranched structures with uncontrollable branching subchains have been extensively prepared and used for the structure−property investigation.[1−7] This is due to the fact that the preparation of an ideal model hyperbranched structure with uniform and adjustable subchains between any two neighboring branching points is rather difficult because of synthetic methodology limitation,[8,9] which seriously hinders the relevant structure−property study.[10,11] Recently, using a novel seesaw-type macromonomer B~~A~~B as the precursor in self-polycondensation reaction, where the reactive A and the two B groups are located at the chain center and the two chain ends, respectively,[12−14] we have successfully prepared model hyperbranched chains. Moreover, we have experimentally, *for the first time*, established the scaling laws between their sizes (R), intrinsic viscosities ($[\eta]$), and molar masses (M);[13,15] found how these chains pass through a small cylindrical nanopore under an elongational flow field;[16,17] and prepared amphiphilic hyperbranched block copolymer chains and studied their interchain and intrachain association in dilute and semidilute solutions.[18]

On the other hand, it is well-known that disulfide bonds can be cleaved into thiol groups in the presence of various reducing agents,[19] such as thiols,[20] phosphines,[21,22] and zinc dust;[23] and the resulting thiol groups can reversibly re-form disulfide bonds upon oxidation. Therefore, the thiol−disulfide exchange reaction has been widely used in various applications, such as drug delivery,[24] gene transfection,[25] and construction of self-healing materials.[26,27] Meanwhile, a number of disulfide-functionalized polymer structures have been prepared, namely, linear (diblock[24,28−30] and multiblock[31,32]), cyclic,[31] comb-like,[33] hyperbranched,[25,34−38] and cross-linking[39−41] structures.

Generally, two main approaches have been used to introduce disulfide linkage into the polymer backbone: (1) homopolymerization of star precursors with thiol ends (Scheme 1A)[31,37] or (2) copolymerization of star precursors with disulfide-functionalized linear small molecules (Scheme 1B).[25,34−36] However, the distributions of the subchain length and disulfide bond location of hyperbranched polymers prepared by these two approaches will be only partly controllable (star precur-

Scheme 1. Schematic of Topological Structures of Disulfide-Functionalized Hyperbranched Chains Prepared by Two Different Approaches: (A) Homopolymerization of Telechelic Star Precursors with Thiol End Groups and (B) Copolymerization of Disulfide-Functionalized Small Molecules and Star Chains
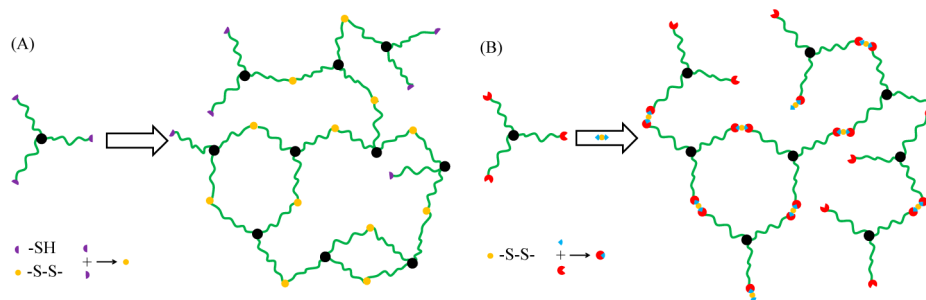
sors).[25,33,34,36,42,43] To the best of our knowledge, it remains a challenge to prepare model hyperbranched polymers with uniform subchains and controlled locations of cleavable disulfide linkages simultaneously.

In the current study, applying our seesaw-type macro-monomer strategy, we have successfully synthesized model hyperbranched polystyrene chains with uniform subchains and controllably located cleavable disulfide linkages. As shown in Scheme 2, seesaw-type macromonomer $\equiv-S-S-(PS-N_3)_2$

Scheme 2. Schematic of Synthesis of Disulfide-Functionalized Seesaw-Type Initiator and Linear Polystyrene Macromonomer $\equiv-S-S-(PS-N_3)_2$
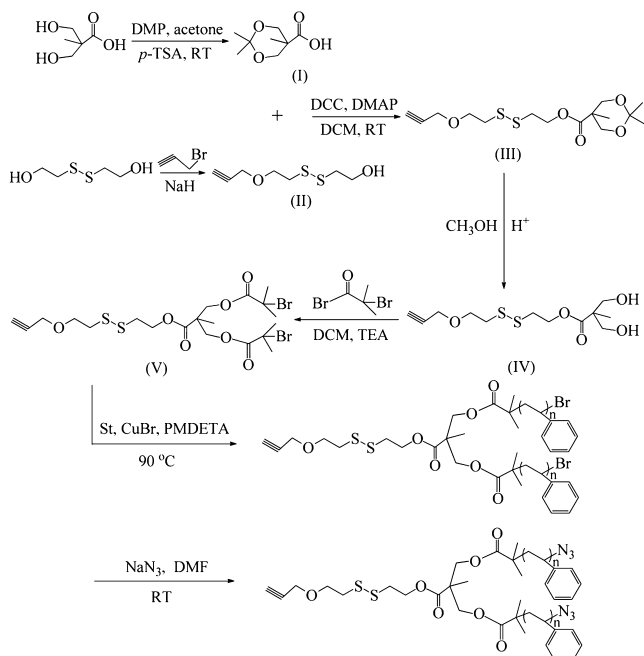
with one disulfide linkage at the chain center was first prepared by atom transfer radical polymerization (ATRP) and azidation substitution reaction. Further interchain "clicking" coupling of macromonomers $\equiv-S-S-(PS-N_3)_2$ led to disulfide-functionalized hyperbranched polystyrene chains (Scheme 3). The well-defined structures of macromonomer and hyperbranched product were confirmed by various kinds of methods. Finally, the degradation kinetics of hyperbranched polystyrene chains in various organic solvents was monitored by a combination of static and dynamic laser light scattering.

Scheme 3. Schematic of Synthesis and Degradation of Disulfide-Functional Hyperbranched Polystyrene Chains $HB-(S-S-PS)_n$
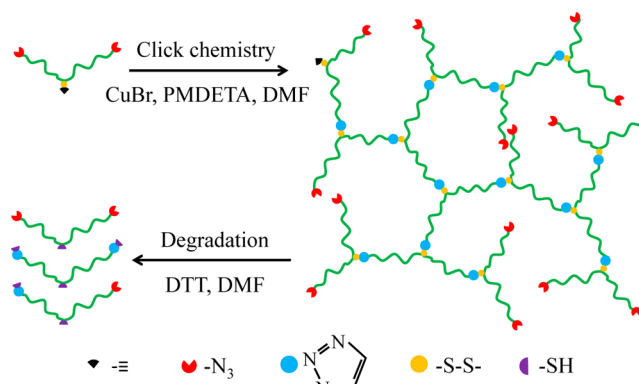
EXPERIMENTAL SECTION

Materials. Styrene (Sinopharm, 97%) was purified by first passing it through a basic alumina column and then distilling under a reduced pressure over calcium hydride (CaH_2). Dimethylformamide (DMF, Sinopharm, AR) was first dried with anhydrous magnesium sulfate and then distilled under a reduced pressure. N,N,N',N',N''-Pentamethyl-diethylenetriamine (PMDETA, Aldrich, 99%), tetrahydrofuran (THF), dichloromethane (DCM), and triethylamine (TEA) were distilled over CaH_2. DMF, THF, and DCM were bubbled with nitrogen for 5 h before used. Dithiothreitol (DTT, Aladdin, 99%) was stored under nitrogen atmosphere at 2−6 °C. All the other reagents from Sinopharm or Aldrich were directly used as received unless otherwise stated.

Characterization. [1]H nuclear magnetic resonance (^{1}H NMR) spectra were recorded using a Bruker AV400 spectrometer with tetramethylsilane (TMS) as an internal standard and deuterated chloroform ($CDCl_3$) as solvent. Fourier transform infrared spectra (FTIR) were recorded using a Bruker VECTOR-22 IR spectrometer, and each spectrum was collected over 64 scans with a spectral resolution of 4 cm^{-1}.

Size Exclusion Chromatography (SEC). The relative number- and weight-average molar masses ($M_{n,RI}$ and $M_{w,RI}$) and the absolute number- and weight-average molar masses ($M_{n,MALLS}$ and $M_{w,MALLS}$) were determined at 35 °C by size exclusion chromatography (SEC, Waters 1515) equipped with three Waters Styragel columns (HR2, HR4, and HR6), a refractive index detector (RI, Wyatt WREX-02), and a multiangle laser light scattering detector (MALLS, Wyatt DAWN EOS). THF was used as the eluent at a flow rate of 1.0 mL/min, and linear narrowly distributed polystyrenes were used as standards.

Laser Light Scattering (LLS). A commercial LLS spectrometer (ALV/DLS/SLS-5022F) equipped with a multi-τ digital time correlator (ALV5000) and a cylindrical 22 mW UNIPHASE He−Ne

laser (λ_0 = 632.8 nm) was used as the light source. In static LLS,[44,45] the angular dependence of the absolute excess time-average scattering intensity, known as the Rayleigh ratio $R_{VV}(q)$, can lead to the weight-average molar mass (M_w), the root-mean-square gyration radius ($\langle R_g \rangle$), and the second virial coefficient A_2 by using

$$\frac{KC}{R_{VV}(q)} \cong \frac{1}{M_w}\left(1 + \frac{1}{3}\langle R_g^2 \rangle_Z q^2\right) + 2A_2C \qquad (1)$$

where $K = 4\pi^2 n^2 (\mathrm{d}n/\mathrm{d}C)^2/(N_A \lambda_0^4)$ and $q = (4\pi n/\lambda_0)\sin(\theta/2)$ with n, C, $\mathrm{d}n/\mathrm{d}C$, N_A, and λ_0 being the refractive index, the concentration of the polymer solution, the specific refractive index increment, Avogadro's number, and the wavelength of light in a vacuum, respectively. The $\mathrm{d}n/\mathrm{d}C$ value of polystyrene in THF is 0.186 mL/g.[12,13]

In dynamic LLS,[46] the Laplace inversion of each measured intensity−intensity time correlation function $G^{(2)}(q,t)$ in the self-beating mode can result in a line-width distribution $G(\Gamma)$. $G(\Gamma)$ can be converted to a translational diffusion coefficient distribution $G(D)$ or further to a hydrodynamic radius distribution $f(R_h)$ via the Stokes−Einstein equation, $R_h = (k_B T/6\pi\eta_0)/D$, where k_B, T, and η_0 are the Boltzmann constant, the absolute temperature, and the solvent viscosity, respectively, by using both the cumulants and CONTIN analysis.

Synthesis of Intermediate Compound I. The general procedure was outlined as follows. 30.0 g of 2,2-bis(hydroxymethyl)propionic acid (223.7 mmol), 41.4 mL of 2,2-dimethoxypropane (DMP) (335.4 mmol), and 2.1 g of *p*-toluenesulfonic acid monohydrate (*p*-TSA, 11.1 mmol) were dissolved in 100 mL of acetone. The mixture was stirred for 4 h at room temperature before a 3.0 mL mixture of an ammonia aqueous solution (25%) and ethanol (50/50, v/v)) was added into the reaction mixture to neutralize the catalyst. The solvent was removed by evaporation under a reduced pressure at room temperature. The residue was then dissolved in DCM (600 mL) and extracted with two portions of water (80 mL). The organic phase was dried with anhydrous Na_2SO_4 and then evaporated to give white powder (33.0 g, 84%). Its ^{1}H NMR spectrum in $CDCl_3$ can be found elsewhere.[47]

Synthesis of Intermediate Compound II. The general procedure was outlined as follows. 20.0 g of 2-hydroxyethyl disulfide (130 mmol) and 3.6 g of propargyl bromide (65 mmol) were mixed in 200 mL of THF. 3.0 g of NaH powder (80 wt %, 98 mmol) was added into the reaction mixture in three successive batches under nitrogen within 3 h at 0 °C. The mixture was further stirred for another 7 h at room temperature before a few drops of water were added to stop the reaction. The mixture was filtered, and the solvent was removed by evaporation under a reduced pressure at 50 °C. The crude product was purfied by column chromatography to give a pale-yellow clear oil: 6.5 g (52%). Figure 1A shows its ^{1}H NMR spectrum in $CDCl_3$. ^{1}H NMR ($CDCl_3$, ppm): δ 4.20 (d, 2H, CH≡CCH_2O−), 3.90 (t, 2H, CH≡CCH_2OCH_2−), 3.81 (t, 2H, −CH_2OH), 2.93 (t, 2H, CH≡CCH_2OCH_2CH_2−), 2.88 (t, 2H, −CH_2CH_2OH), 2.46 (t, 1H, CH≡CCH_2−), 1.93 (s, 1H, −CH_2OH).

Synthesis of Intermediate Compound III. The general procedure was outlined as follows. 5.4 g of compound I (31.3 mmol), 6.0 g of compound II (31.3 mmol), and 0.38 g of 4-(dimethylamino)pyridine (DMAP) (3.1 mmol) were dissolved in 100 mL of DCM. 7.74 g of *N,N'*-dicyclohexylcarbodiimide (DCC) (37.6 mmol) was dissolved in 50 mL of DCM. The two solutions were mixed under nitrogen flow at 0 °C within 0.5 h and further stirred overnight at room temperature. The byproduct *N,N'*-dicyclohexylurea was filtered. The solution was then diluted by 100 mL of DCM and extracted with two portions of water (150 mL). The organic phase was dried with anhydrous sodium sulfate. After removing the solvent by evaporation, the crude product was purified by column chromatography to give a pale-yellow oil: 8.0 g (83%). Figure 1B shows its ^{1}H NMR spectrum in $CDCl_3$. ^{1}H NMR ($CDCl_3$, ppm): δ 4.43 (t, 2H, CH≡CCH_2O−), 4.20 (m, 4H, $(CH_3)_2$C(OCH_2−)), 3.79 (t, 2H, −CH_2OOC−), 3.66 (m, 2H, CH≡CCH_2OCH_2−), 2.96 (m, 4H, −CH_2SSCH_2−), 2.46 (t, 1H, CH≡CCH_2−), 1.40 (m, 6H, $(CH_3)_2$C(OCH_2−)), 1.21 (s, 3H, CH_3−).
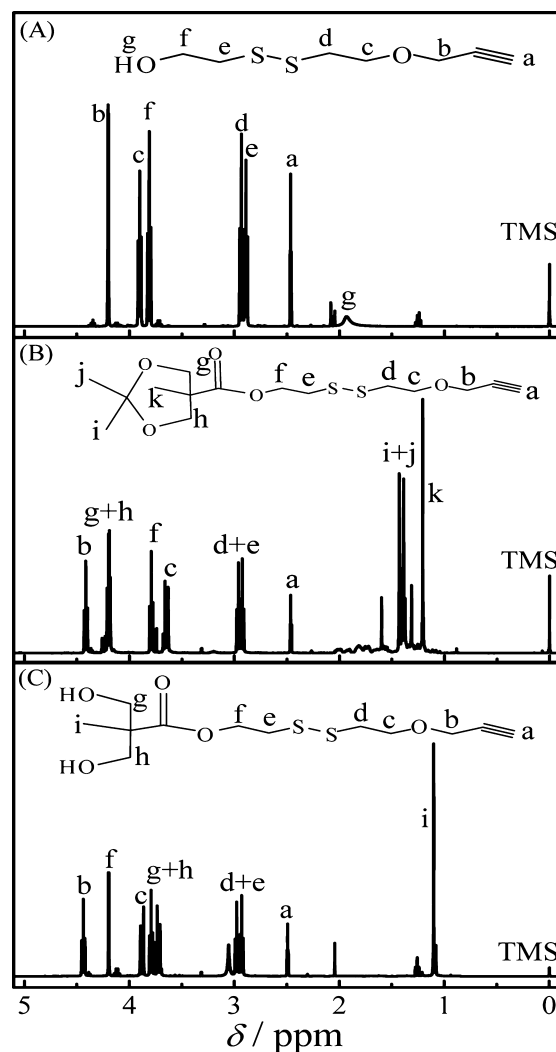

Figure 1. ^{1}H NMR spectra of the intermediate compounds (**II−IV**) in $CDCl_3$.

Synthesis of Intermediate Compound IV. The general procedure was outlined as follows. 8.0 g of compound III (25.0 mmol) dissolved in 100 mL of methanol was added with an excess of activated acidic styrene cation exchange resin (Amberlite IR-120, aladdin). The mixture was stirred for 4 h at room temperature. After the resin was filtered, the solvent was removed by evaporation. The crude product was purified by column chromatography to give a pale-yellow oil: 7.1 g (89%). Figure 1C shows its ^{1}H NMR spectrum in $CDCl_3$. ^{1}H NMR ($CDCl_3$, ppm): δ 4.45 (t, 2H, CH≡CCH_2O−), 4.20 (t, 2H, −CH_2OOC−), 3.88 (d, 2H, CH≡CCH_2OCH_2−), 3.75 (m, 4H, HOCH_2−), 2.95 (m, 4H, −CH_2SSCH_2−), 2.46 (t, 1H, CH≡CCH_2−), 1.11 (s, 3H, CH_3−).

Synthesis of Compound V, Seesaw-Type Initiator. The general procedure was outlined as follows. 6.5 g of compound IV (21.1 mmol) and 2.6 g of TEA (25.3 mmol) were dissolved in 150 mL of DCM. 11.6 g of α-bromoisobutyryl bromide (50.6 mmol) dissolved in 50 mL of DCM was added into the reaction mixture under nitrogen flow at 0 °C within 0.5 h. The mixture was stirred overnight. After filtration, the mixture was diluted with 100 mL of DCM and extracted with 50 mL of saturated sodium bicarbonate aqueous solution. The organic phase was dried with anhydrous sodium sulfate. After removing the solvent by evaporation, the crude product was purified by column chromatography to give a dark-yellow oil: 9.0 g (71%). Figure 2 shows its ^{1}H NMR spectrum in $CDCl_3$. ^{1}H NMR ($CDCl_3$, ppm): δ 4.43 (m, 4H, $(COOCH_2)_2CCH_3$−), 4.38 (t, 2H, CH≡CCH_2O−), 4.20 (t, 2H, −CH_2OOCSS−), 3.80 (m, 2H, CH≡CCH_2OCH_2−), 2.95 (m, 4H,
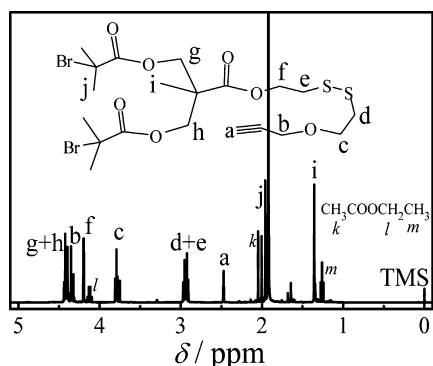
Figure 2. ¹H NMR spectrum of disulfide-functionalized initiator.

−CH₂SSCH₂−), 2.48 (t, 1H, CH≡CCH₂−), 1.98 (d, 12H, BrC(CH₃)₂−), 1.36 (s, 3H, CH₃−).

Preparation of Macromonomer ≡−S−S−(PS−Br)₂ by ATRP. The general procedure was outlined as follows. A three-necked flask equipped with a magnetic stirring bar and three rubber septa was charged with 0.4 g of initiator **V** (0.66 mmol), 12.1 mL of styrene (105.9 mmol), and 124 μL of PMDETA (0.66 mmol). The flask was degassed by three freeze−pump−thaw cycles and then placed in an oil bath thermostated at 90 °C. After ∼2 min, 93.7 mg of CuBr (0.66 mmol) was added under nitrogen flow to start the polymerization. Samples were withdrawn at different times during the polymerization for SEC and monomer conversion measurements by the weighing method. Namely, the conversion was calculated as conversion = m/m_0, where m_0 and m represent the weights of sample solution before and after removing styrene monomer by evaporation under a reduced pressure at 50 °C for four cycles; in each cycle, a certain amount of THF was added to enhance the extraction of styrene. After a few hours, the flask was rapidly cooled in liquid nitrogen. The polymer mixture was diluted with THF and passed through a short column of neutral alumina to remove metal salt. The solvent was removed by evaporation, and the residue was dissolved in THF and precipitated into an excess of methanol and recovered by filtration. The above purification cycle was repeated twice. After drying in a vacuum oven overnight at 40 °C, macromonomer ≡−S−S−(PS−Br)₂ was obtained. Yield: 6.15 g (54%). M_n: 9.4 × 10³ g/mol and M_w/M_n: 1.14 (by SEC); M_n: 9.0 × 10³ g/mol (by ¹H NMR in Figure 2).

Preparation of Macromonomer ≡−S−S−(PS−N₃)₂ by Azidation. The general procedure was outlined as follows. A 100 mL round-bottom flask was charged with 5.0 g of ≡−S−S−(PS−Br)₂ (0.45 mmol), 40 mL of DMF, and 0.29 g of sodium azide (4.5 mmol). The mixture was allowed to stir at room temperature for 24 h under nitrogen flow. After removing DMF under a reduced pressure, the remaining portion was diluted with DCM and passed through a neutral alumina column to remove residual sodium salts. The solvent was removed by evaporation, and the residue was dissolved in THF and precipitated into an excess of methanol. After drying in a vacuum oven overnight at 40 °C, azido-terminated polymer was obtained and named as ≡−S−S−(PS−N₃)₂. Yield: 4.7 g (94%). M_n: 9.3 × 10³ g/mol and M_w/M_n: 1.12 (by SEC).

Preparation of Degradable Hyperbranched Polymer HB-(S−S−PS)ₙ by "Click" Chemistry. The general procedure was outlined as follows. A 25 mL three-necked flask equipped with a magnetic stirring bar and three rubber septa was charged with 4.5 g of macromonomer ≡−S−S−(PS−N₃)₂ (∼0.43 mmol, $M_{w,macromonomer}$ = 1.04 × 10⁴ g/mol), 83 μL of PMDETA (0.40 mmol), and 15.0 mL of DMF. The flask was degassed by three freeze−pump−thaw cycles and then placed in a water bath thermostated at 35 °C. After ∼2 min, 57.5 mg of CuBr (0.40 mmol) was added under nitrogen flow to start the polymerization. Samples were withdrawn at different times and precipitated into a mixture of methanol/water (90/10, v/v) for SEC measurements. After 24 h, the flask was cooled in liquid nitrogen. The polymer mixture was diluted with THF and passed through a short column of neutral alumina for the removal of metal salt. The solvent was

removed by evaporation, and the residue was dissolved in THF and precipitated into an excess of methanol. After drying in a vacuum oven overnight at 40 °C, hyperbranched polymer HB-(S−S−PS)ₙ was obtained. The resultant polydispersed HB-(S−S−PS)ₙ was further purified by fractional precipitation in a mixed solution of toluene/methanol to remove most of the low-molar-mass fractions. Finally, hyperbranched HB-(S−S−PS)ₙ fraction with a M_w of ∼3.7 × 10⁵ g/mol ($n \simeq 35$) was obtained and used in the degradation kinetics study.

DTT-Induced Degradation of HB-(S−S−PS)₃₅ Chains. The DTT-induced degradation of HB-(S−S−PS)₃₅ was conducted *in situ* inside the LLS cuvette. Stock DMF solutions of HB-(S−S−PS)₃₅ (1.0 g/L) and DTT (25.0 g/L) were purged by nitrogen to replace oxygen and respectively clarified with 0.45 μm Millipore PTFE filters to remove dust. In a typical experiment, a proper amount of dust-free DTT DMF solution was rapidly added into 3.0 mL of dust-free HB-(S−S−PS)₃₅ DMF solution to start the degradation. Both the scattered intensity and $G^{(2)}(q,t)$ were recorded during the degradation for at least 1000 min.

■ RESULTS AND DISCUSSION

As shown in Scheme 2, disulfide-functional initiator (**V**) was prepared through a five-step synthesis. All the intermediate compounds (**II−IV**) were carefully purified by column chromatography, and their high purities were confirmed by ¹H NMR characterization (Figure 1A−C).

Figure 2 shows the ¹H NMR spectrum of the tetrafunctional initiator, and the integral area ratio of peak (*a*), peak (*i*), and peak (*d* + *e*) is 1.00/3.10/4.09, in consistency with its theoretical ratio of 1.00/3.00/4.00. Using this functional initiator, seesaw-type polystyrene macromonomer ≡−S−S−(PS−Br)₂ was successfully prepared by ATRP, and its typical ¹H NMR spectrum is shown in Figure 3.

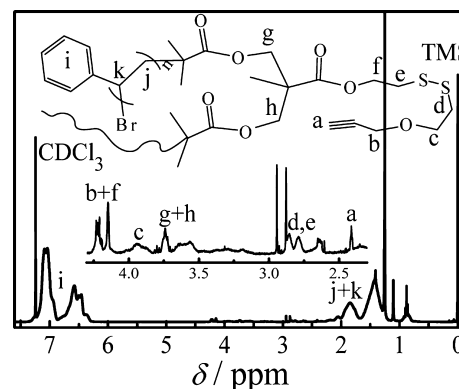**Figure 3.** ¹H NMR spectrum of disulfide-functionalized ≡−S−S−(PS−Br)₂.

Figures 4−6 show how the monomer conversion, number-average molar mass (M_n), polydispersity index (M_w/M_n), and SEC curves of polystyrene evolved during the ATRP process. As shown in Figure 4, the plot of semilogarithmic of ln(1/(1 − conversion)) versus *t* presents a linear relation, indicating the polymerization meets the required criteria of a living system. Figure 5 shows that the experimental M_n increases linearly with the conversion, and the M_w/M_n rapidly decreases with the conversion and reaches a minimum of ∼1.14 at the end of polymerization, indicating the whole ATRP process is well-controlled, which is also reflected in the symmetric and narrowly distributed elution curves (Figure 6).

In a typical ATRP process, the molar ratio of CuBr to halogen atom on initiator is normally 1.0/1.0, while the ratio in
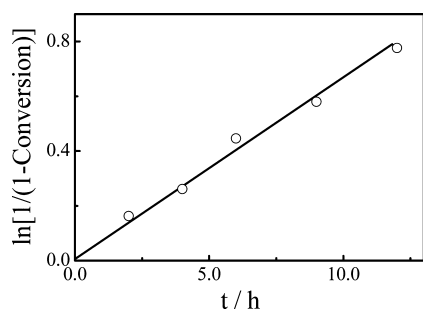
Figure 4. (A) Kinetic plot of semilogarithmic of $\ln(1/(1 - \text{conversion}))$ versus reaction time (t) during the ATRP process. Reaction conditions: [styrene]/[initiator]/[CuBr]/[PMDETA] = 150/1/1/1; T = 90 °C; bulk.
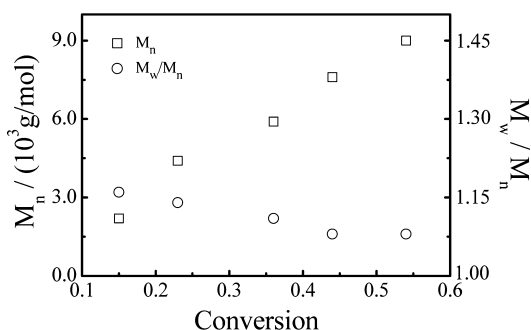

Figure 5. Monomer conversion dependence of number-average molar mass (M_n) and polydispersity index (M_w/M_n) of macromonomer $\equiv$–S–S–(PS–Br)$_2$ during the ATRP process. Reaction conditions: [styrene]/[initiator]/[CuBr]/[PMDETA] = 150/1/1/1; T = 90 °C; bulk.
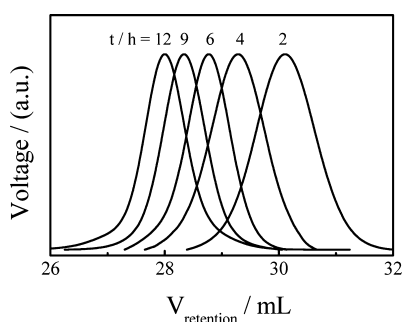

Figure 6. Reaction time (t)-dependent SEC curves of macromonomer $\equiv$–S–S–(PS–Br)$_2$ during the ATRP process. Reaction conditions: [styrene]/[initiator]/[CuBr]/[PMDETA] = 150/1/1/1; T = 90 °C; bulk.

our study is actually 1.0/0.5. In addition, the monomer conversion was intentionally controlled below 60%, which is because both the CuBr concentration and monomer conversion are the key factors to attain polymer chains with high end-group functionalities. In principle, lowering both the CuBr concentration and monomer conversion can effectively reduce the chain termination and other side reactions.[48,49]

Further azidation substitution reaction of $\equiv$–S–S–(PS–Br)$_2$ by sodium azide in DMF led to macromonomer $\equiv$–S–S–(PS–N$_3$)$_2$. The successful installation of azide groups was reflected in the appearance of a N$\equiv$N$\equiv$N antisymmetric stretching absorption band near ~2090 cm^{-1} in FT-IR spectra (Figure 7). Using this seesaw-type macromonomer $\equiv$–S–S–(PS–N$_3$)$_2$, we are able to prepare degradable hyperbranched
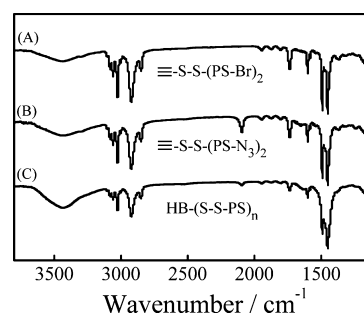

Figure 7. IR spectra of (A) $\equiv$–S–S–(PS–Br)$_2$, (B) $\equiv$–S–S–(PS–N$_3$)$_2$, and (C) HB-(S–S–PS)$_n$.

polystyrene chains with uniform subchains and controlled locations of cleavable disulfide linkages. Scheme 3 schematically shows the structures of the prepared hyperbranched chains and its degradation products.

The alkyne–azide "click" cycloaddition was used here because of its high efficiency and low susceptibility to side reactions.[50–52] DMF was used as solvent in the interchain "clicking" of macromonomer $\equiv$–S–S–(PS–N$_3$)$_2$ after the removal of oxygen at 35 °C with a catalyst of CuBr–PMDETA. Similar to our previous study,[12,13] we prefer to use the weight-average polycondensation degree (DP$_w$), instead of the number-average polycondensation degree (DP$_n$), to describe the whole interchain "clicking" process because it is the weight-average value that could be measured accurately in SEC-MALLS or stand-alone static LLS, where DP is defined as the number of macromonomers, not monomer, chemically coupled together inside each hyperbranched polystyrene chain; namely, DP$_w$ = $M_{w,\text{hyperbranched}}/M_{w,\text{macromonomer}}$ ($M_{w,\text{macromonomer}} = 1.04 \times 10^4$ g/mol).

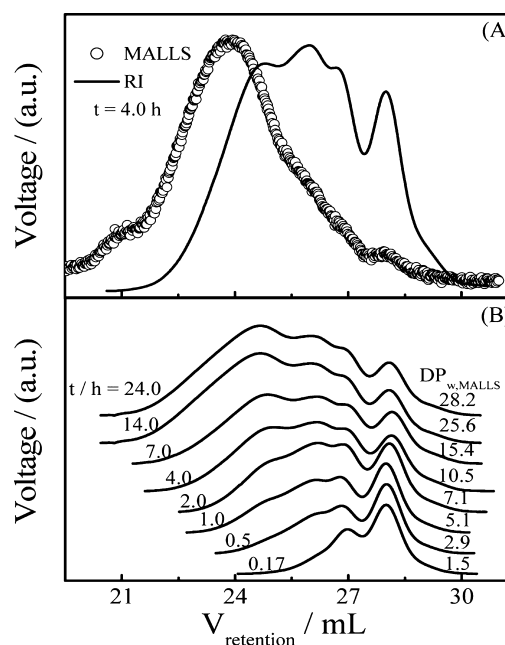Figure 8A shows that the two elution curves respectively from the RI and MALLS detectors are very different. This is

Figure 8. (A) Comparison of two typical SEC curves of HB-(S–S–PS)$_n$ monitored by two different detectors: RI (solid line) and MALLS (circle symbol) and (B) reaction time (t)-dependent SEC-RI curves of HB-(S–S–PS)$_n$, where T = 35 °C and C_{polymer} = 0.30 g/mL.

because the scattered light intensity in LLS is proportional to the product of the weight-average molar mass and the weight concentration, while the signal from RI is only proportional to the weight concentration. Figure 8B shows the reaction time-dependent SEC curves of HB-(S−S−PS)$_n$ during the self-polycondensation. As the reaction proceeds, the macromonomer peak becomes smaller while the hyperbranched polymer peaks emerged after a few hours. Gradually, DP$_w$ and DP$_n$ increase to ∼28 and ∼6, respectively, and its polydispersity index (M_w/M_n) changes from 1.14 to 4.90 (Figure 9) when
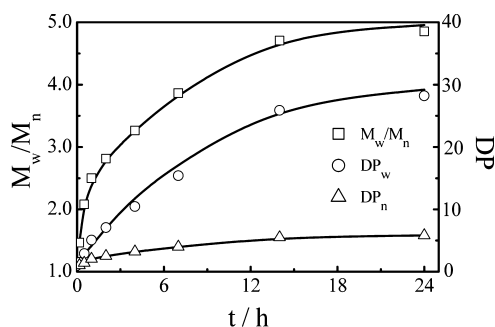

Figure 9. Reaction time (t) dependence of polydispersity index (M_w/M_n), number (DP$_n$), and weight-average degree of polycondensation (DP$_w$) of HB-(S−S−PS)$_n$, where T = 35 °C and $C_{polymer}$ = 0.30 g/mL.

most of the initial macromonomers are coupled together, reflecting in a sharp decrease of the N=N=N stretching absorption near ∼2100 cm^{-1} (Figure 7C). The self-polycondensation nearly ceases after ∼14 h, similar to what we observed in a previous study.[13] The related polycondensation kinetics analysis can be found elsewhere.[13]

As discussed before, each branching point of HB-(S−S−PS)$_n$ contains just one disulfide bond that is cleavable when a reducing agent is added. The cleavage of each disulfide bond results in two smaller fragemented hyperbranched chains with a thiol end group. Using a combination of static and dynamic LLS, we studied such a degradation kinetics of a fractionated HB-(S−S−PS)$_n$ with a DP$_w$ of 35 and a M_w/M_n of 1.40. There are different choices of reducing reagents, including thiols,[20] phosphines,[21,22] and zinc dust.[23] DTT was selected in the current study because (1) its induced disulfide reduction is very efficient owing to its high conformational propensity to form a six-member ring with an internal disulfide bond and (2) it is soluble in a range of organic solvents that can also dissolve polystyrene easily.[28]

Figures 10 and 11 show how HB-(S−S−PS)$_{35}$ chains change after the 24 h DTT induced reduction in DMF at 25 °C. As shown in Figure 10, the elution peak located at ∼24 mL completely disappears after the degradation, and only the macromonomer peak (maybe contains few dimers) remains, indicating that the DTT induced degradation of the initial HB-(S−S−PS)$_{35}$ chains is nearly 100%. The residual dimers are attributed to the limited degradation time (24 h). Such chain degradation is also directly reflected in the evolution of the hydrodynamic radius distribution [$f(R_h)$], as shown in Figure 11; i.e., the peak position shifts from ∼19 to ∼3 nm after degradation. However, it should be noted that the degradation products are similar to the initial seesaw-type linear macromonomers except different end groups, as shown in Scheme 3.

Figure 12 shows how the DP$_w$, $\langle R_h \rangle$, and average chain density ($\langle \rho \rangle$) of HB-(S−S−PS)$_{35}$ change during the degrada-
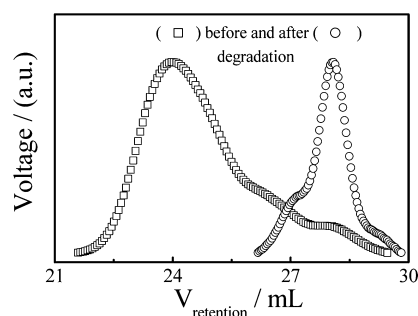

Figure 10. SEC-RI curves of HB-(S−S−PS)$_{35}$ chains before and after 24 h DTT-induced reduction in DMF at 25 °C, where [DTT]/[−S−S−] = 18.
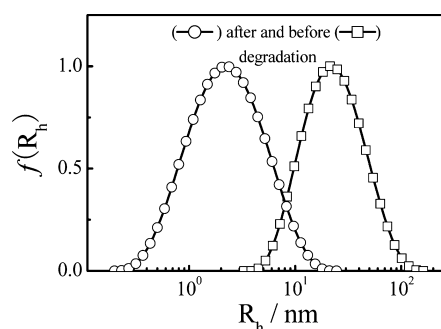

Figure 11. Hydrodynamic radius distributions [$f(R_h)$] of HB-(S−S−PS)$_{35}$ chains before and after 24 h DTT-induced reduction in DMF at 25 °C, where [DTT]/[−S−S−] = 18.

tion at different molar ratios of [DTT]/[−S−S−]; for the convenience of discussion, DP$_{w,t}$ is used to represent the value of DP$_w$ at time t. As expected, DP$_{w,t}$ and $\langle R_h \rangle$ gradually decrease as the degradation (fragmentation) proceeds for a given [DTT]/[−S−S−], and the degradation rate becomes higher when more DTT is added. We tested whether all the disulfide bonds can be completely degraded in the range of [DTT]/[−S−S−] = 3−180 and found that most of the initial disulfide bonds were cleaved within 5 h even at [DTT]/[−S−S−] = 3. Figure 12C shows that the average chain density ($\langle \rho \rangle$), defined as $M_w/[N_A(4/3)\pi\langle R_h \rangle^3]$, increases with the degradation time, where M_w, $\langle R_h \rangle$, and N_A are the weight-average molar mass, the average hydrodynamic radius of hyperbranched chains, and Avogadro's number, respectively, revealing that larger branched chains have a lower chain density than its degraded products and the initial linear macromonomer has the highest $\langle \rho \rangle$.

To analyze the results in Figure 12, and considering the nature of thiol−disulfide exchanging reaction, we first assumed that the degradation follows the second-order kinetics, i.e.

$$-\frac{d[-S-S-]_t}{dt} = k[-S-S-]_t[DTT]_t \tag{2}$$

where $[-S-S-]_t$ and $[DTT]_t$ are the molar concentrations of disulfide bond and DTT at time t, respectively, and k is a reaction rate constant. At $t = 0$, $[-S-S-]_t = [-S-S-]_0$, and at $t = \infty$, $[-S-S-]_t = 0$. Since DTT is excessive, we can treat $[DTT]_t = [DTT]_0$ as a constant in eq 2 so that we can rewrite it as a pseudo-first-order equation

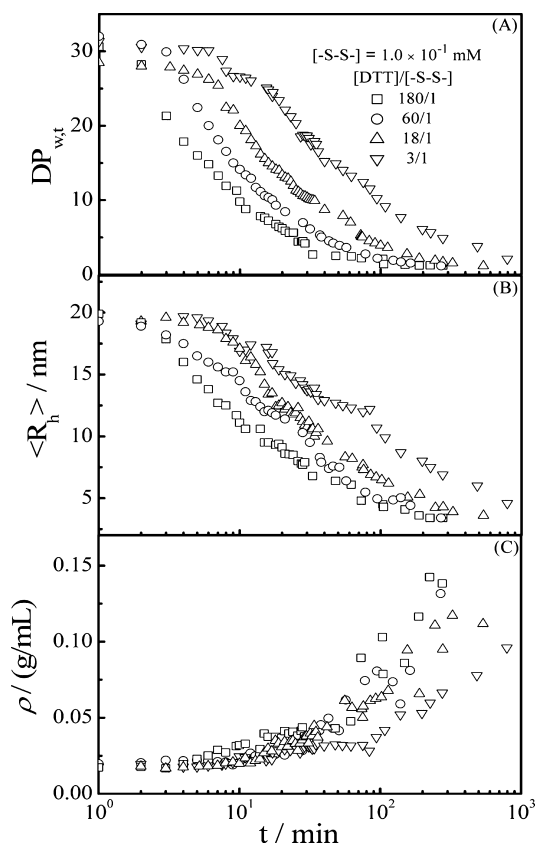$$\frac{[-S-S-]_t}{[-S-S-]_0} = e^{-k[DTT]_0 t} \tag{3}$$

Figure 12. Degradation time (t) dependence of (A) weight-average degree of polycondensation ($DP_{w,t}$), (B) average hydrodynamic radius ($\langle R_h \rangle$), and (C) average chain density ($\langle \rho \rangle$) of HB-$(S-S-PS)_{35}$ in DMF at 25 °C.

On the other hand, it is well-known that polystyrene is insoluble in diols so that most of DTT are excluded from the interior of HB-$(S-S-PS)_n$. Therefore, those external disulfide bonds would be cleaved first. As shown in Scheme 3, the cleavage of each external disulfide bond leads to a decrease of DP_w by one. In this way, we are able to rewrite $[-S-S-]_t / [-S-S-]_0$ as $DP_{w,t}/DP_{w,0}$ so that eq 3 can be rewritten as

$$DP_{w,t} = DP_{w,0}e^{-Kt} \qquad (4)$$

where $DP_{w,t}$ and $DP_{w,0}$ are the degrees of polycondensation of hyperbranched chains at $t = t$ and $t = 0$, respectively, and $K = k[DTT]_0$.

However, Figure 13A shows that the single-exponential fitting using eq 3 is not satisfactory, which forces us to include the degradation of those disulfide bonds inside the hyperbranched polystyrene chain. It is expected that the degradation of those internal disulfide bonds would be much slower due to (1) the lower concentration of DTT inside the polystyrene core and (2) the steric effect of the polystyrene segments around each internal disulfide bond. Empirically, we found that adding a slow degradation process into eq 4 enables us to fit all the curves in Figure 13B by using a double-exponential fitting as follows:

$$\frac{DP_{w,t}}{DP_{w,0}} = A_{fast}e^{-K_{fast}t} + A_{slow}e^{-K_{slow}t} \qquad (5)$$

where A and K are two constants, representing the relative contributions and rate constants of the slow and fast
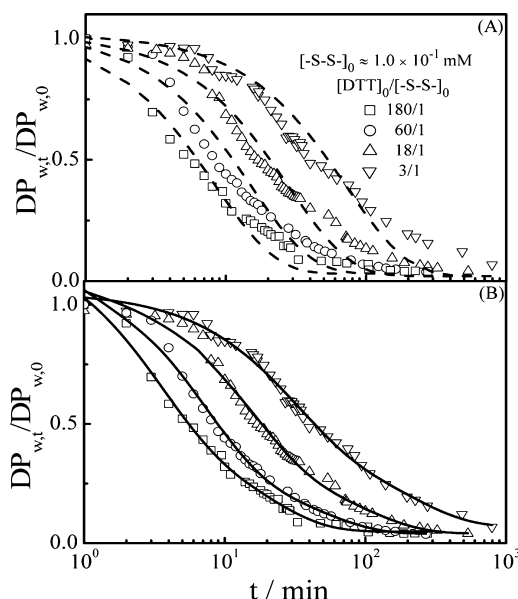

Figure 13. DTT-induced degradation time (t) dependence of normalized weight-average degree of polycondensation ($DP_{w,t}/DP_{w,0}$) of HB-$(S-S-PS)_{35}$ in DMF at 25 °C, where dashed and solid lines represent a single-exponential fitting (eq 4) and a double-exponential fitting (eq 5), respectively.

degradation reactions, respectively; $A_{fast} + A_{slow} = 1.0$. The reasonable double-exponential fitting actually reveals that the degradation of disulfide bonds on the periphery of the hyperbranched chain is much faster than those inside.

Moreover, Figure 14A shows that the fast degradation contributes twice more than the slow one; namely, ~2/3 of the disulfide bonds are on the periphery. It is interesting to find that the contributions of the fast and slow degradations are independent of the DTT concentration, presumably because
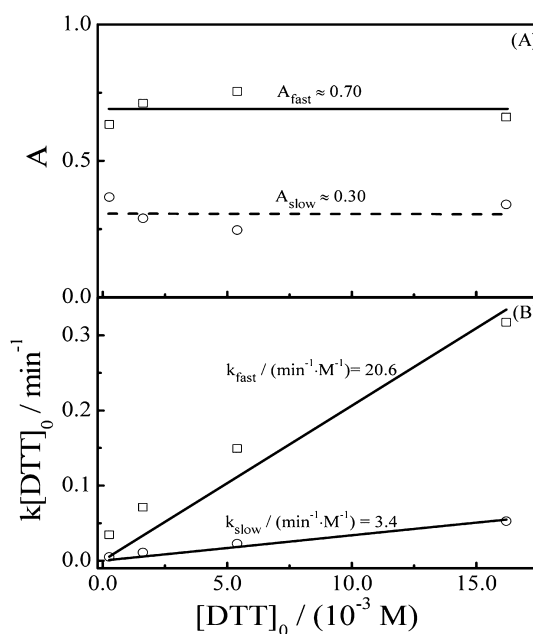

Figure 14. DTT initial concentration ($[DTT]_0$) dependence of (A) relative contributions (A) of fast and slow degradation processes and (B) reaction rate constants k_{fast} and k_{slow} calculated from fitting of data in Figure 13 on the basis of eq 5.

the distribution of the disulfide bonds inside a hyperbranched chain is not influenced by the presence of DTT. In addition, Figure 14B reveals that both K_{fast} and K_{slow} increase linearly with the DTT concentration, i.e., $K_{fast} = k_{fast}[DTT]_0$ and $K_{slow} = k_{slow}[DTT]_0$, indicating that the cleavage of the disulfide bond on a polymer chain by DTT is very similar to those small molecule thiol−disulfide exchange reactions.[53−55] It is worth noting that both k_{fast} and k_{slow} are much smaller than the apparent rate constants $(10^5–10^6 \text{ min}^{-1} \text{ M}^{-1})$ of small molecule thiol−disulfide exchange reactions in DMF.[56]

Finally, we studied the effect of solvent on the degradation kinetics of HB-(S−S−PS)$_{35}$ because it is practically important to choose a proper solvent to degrade a given polymer chain. Figure 15 shows that the degradation rate increases with the
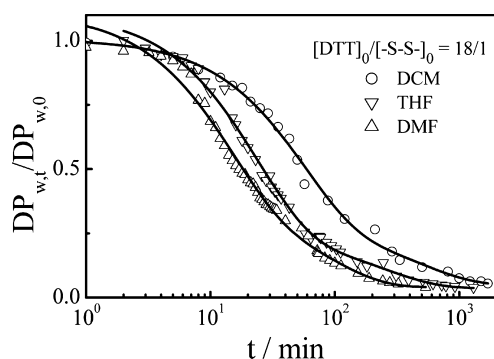

Figure 15. DTT-induced degradation time (t) dependence of normalized weight-average degree of polycondensation (DP$_{w,t}$/DP$_{w,0}$) of HB-(S−S−PS)$_{35}$ in three different solvents at 25 °C, where lines represent double-exponential fittings of eq 5.

solvent polarity. To our knowledge, this is the first study of how the solvent polarity affects the degradation kinetics of disulfide-functionalized hyperbranched polymers. Quatitatively, the fast and slow degradation rate constants in DMF are ∼2 and ∼5 times higher than those in THF and DCM, respectively. It has been known that the reducing power of DTT depends on how easily the thiol groups of DTT are ionized into the thiolate form −S$^-$ because only a free thiolate can attack the disulfide linkage on a chain.[28,52] Generally, organic solvents with a higher polarity are able to polarize the thiol group to produce more free thiolate.

■ CONCLUSION

Using the interchain "clicking" of disulfide-functional macromonomer ≡−S−S−(PS−N$_3$)$_2$, we have successfully prepared model hyperbranched polystyrene chains with both uniform subchains and controlled locations of cleavable disulfide linkage. The DTT-induced degradation of such model hyperbranched chains in DMF contains a fast and a slow process because the degradation of the disulfide bonds on the chain periphery is much faster than those inside, attributing to a higher DTT concentration outside and a weaker steric effect of the polystyrene segments. Not only the category of monomer and cleavable linkage but also the coupling method developed in the current study can be alternated to make various structure-defined degradable hyperbranched polymer chains, which makes further studies of the correlation between microscopic structures and macroscopic properties of degradable hyperbranched polymers possible. We can envision that such degradable hyperbranched chains can be used to encapsulate active chemicals and release them in a controllable fashion because hyperbranched chains have a smaller size and a less tendency to aggregate with each other than their linear counterparts for a given molar mass.

■ AUTHOR INFORMATION

Corresponding Authors
*E-mail llw@mail.ustc.edu.cn (L.L.).
*E-mail xdye@ustc.edu.cn (X.Y.).

Notes
The authors declare no competing financial interest.

■ ACKNOWLEDGMENTS

■ REFERENCES

(1) Kong, L.; Sun, M.; Qiao, H.; Pan, C. *J. Polym. Sci., Part A: Polym. Chem.* **2010**, *48*, 454.
(2) Liu, D.; Zeng, S.; Hu, Q.; Yi, C.; Xu, Z. *Polym. Bull.* **2010**, *64*, 877.
(3) Xu, J.; Tao, L.; Boyer, C.; Lowe, A. B.; Davis, T. P. *Macromolecules* **2009**, *43*, 20.
(4) Konkolewicz, D.; Gray-Weale, A.; Perrier, S. B. *J. Am. Chem. Soc.* **2009**, *131*, 18075.
(5) Hutchings, L. R. *Soft Matter* **2008**, *4*, 2150.
(6) Hutchings, L. R.; Dodds, J. M.; Roberts-Bleming, S. J. *Macromol. Symp.* **2006**, *240*, 56.
(7) Hutchings, L. R.; Dodds, J. M.; Roberts-Bleming, S. J. *Macromolecules* **2005**, *38*, 5970.
(8) Zimm, B. H.; Stockmayer, W. H. *J. Chem. Phys.* **1949**, *17*, 1301.
(9) de Gennes, P. G. *Biopolymers* **1968**, *6*, 715.
(10) Hutchings, L. R.; Dodds, J. M.; Rees, D.; Kimani, S. M.; Wu, J. J.; Smith, E. *Macromolecules* **2009**, *42*, 8675.
(11) Konkolewicz, D.; Poon, C. K.; Gray-Weale, A.; Perrier, S. *Chem. Commun.* **2010**, *47*, 239.
(12) He, C.; Li, L.; He, W.; Jiang, W.; Wu, C. *Macromolecules* **2011**, *44*, 6233.
(13) Li, L.; He, C.; He, W.; Wu, C. *Macromolecules* **2011**, *44*, 8195.
(14) He, C.; He, W.; Li, L.; Jiang, W.; Tao, J.; Yang, J.; Chen, L.; Ge, X.; Chen, S. *J. Polym. Sci., Part A: Polym. Chem.* **2012**, *50*, 3214.
(15) Li, L.; Lu, Y.; An, L.; Wu, C. *J. Chem. Phys.* **2013**, *138*, 114908.
(16) Li, L.; He, C.; He, W.; Wu, C. *Macromolecules* **2012**, *45*, 7583.
(17) Wu, C.; Li, L. *Polymer* **2013**, *54*, 1463.
(18) Li, L.; Zhou, J.; Wu, C. *Macromolecules* **2012**, *45*, 9391.
(19) Jocelyn, P. C. Chemical reduction of disulfides. In *Methods in Enzymology*; William, B., Jakoby, O. W. G., Eds.; Academic Press: New York, 1987; Vol. *143*, p 246.
(20) Cleland, W. W. *Biochemistry* **1964**, *3*, 480.
(21) Humphrey, R. E.; Hawkins, J. M. *Anal. Chem.* **1964**, *36*, 1812.
(22) Humphrey, R. E.; Potter, J. L. *Anal. Chem.* **1965**, *37*, 164.
(23) Overman, L. E.; Smoot, J.; Overman, J. D. *Synthesis* **1974**, *1974*, 59.
(24) Wang, W.; Sun, H.; Meng, F.; Ma, S.; Liu, H.; Zhong, Z. *Soft Matter* **2012**, *8*, 3949.
(25) Deng, R.; Yue, Y.; Jin, F.; Chen, Y.; Kung, H.-F.; Lin, M. C. M.; Wu, C. *J. Controlled Release* **2009**, *140*, 40.
(26) Canadell, J.; Goossens, H.; Klumperman, B. *Macromolecules* **2011**, *44*, 2536.

(27) Yoon, J. A.; Kamada, J.; Koynov, K.; Mohin, J.; Nicolaÿ, R.; Zhang, Y.; Balazs, A. C.; Kowalewski, T.; Matyjaszewski, K. *Macromolecules* **2011**, *45*, 142.

(28) Tsarevsky, N. V.; Matyjaszewski, K. *Macromolecules* **2002**, *35*, 9009.

(29) Wang, Y.; Wang, F.; Sun, T.; Wang, J. *Bioconjugate Chem.* **2011**, *22*, 1939.

(30) Ko, N. R.; Yao, K.; Tang, C.; Oh, J. K. *J. Polym. Sci., Part A: Polym. Chem.* **2012**, *51*, 3071.

(31) Whittaker, M. R.; Goh, Y.-K.; Gemici, H.; Legge, T. M.; Perrier, S.; Monteiro, M. J. *Macromolecules* **2006**, *39*, 9028.

(32) Zhang, Q.; Noh, S. M.; Nam, J. H.; Jung, H. W.; Park, J. M.; Oh, J. K. *Macromol. Rapid Commun.* **2012**, *33*, 1528.

(33) Zhang, M.; Liu, H.; Shao, W.; Miao, K.; Zhao, Y. *Macromolecules* **2013**, *46*, 1325.

(34) Tsarevsky, N. V.; Huang, J.; Matyjaszewski, K. *J. Polym. Sci., Part A: Polym. Chem.* **2009**, *47*, 6839.

(35) Xu, J.; Tao, L.; Liu, J.; Bulmus, V.; Davis, T. P. *Macromolecules* **2009**, *42*, 6893.

(36) Yang, W.; Pan, C. *Macromol. Rapid Commun.* **2009**, *30*, 2096.

(37) Yan, J.; Hong, C.; You, Y. *Macromolecules* **2011**, *44*, 1247.

(38) Jiang, X.; Zhang, M.; Li, S.; Shao, W.; Zhao, Y. *Chem. Commun.* **2012**, *48*, 9906.

(39) Kamada, J.; Koynov, K.; Corten, C.; Juhari, A.; Yoon, J. A.; Urban, M. W.; Balazs, A. C.; Matyjaszewski, K. *Macromolecules* **2010**, *43*, 4133.

(40) Steinhauer, W.; Keul, H.; Moller, M. *Polym. Chem.* **2011**, *2*, 1803.

(41) Zhang, Q.; Aleksanian, S.; Noh, S. M.; Oh, J. K. *Polym. Chem.* **2013**, *4*, 351.

(42) Tao, L.; Liu, J.; Tan, B. H.; Davis, T. P. *Macromolecules* **2009**, *42*, 4960.

(43) You, Y.; Hong, C.; Pan, C. *Macromolecules* **2009**, *42*, 573.

(44) Zimm, B. H. *J. Chem. Phys.* **1948**, *16*, 1099.

(45) Chu, B. *Laser Scattering*, 2nd ed.; Academic Press: New York, 1991.

(46) Berne, B.; Pecroa, R. *Dynamic Light Scattering*; Plenum Press: New York, 1976.

(47) Li, L.; Yan, M.; Zhang, G.; Wu, C. *Macromolecules* **2013**, *46*, 8152.

(48) Lutz, J. F.; Matyjaszewski, K. *J. Polym. Sci., Part A: Polym. Chem.* **2005**, *43*, 897.

(49) Jakubowski, W.; Kirci-Denizli, B.; Gil, R. R.; Matyjaszewski, K. *Macromol. Chem. Phys.* **2008**, *209*, 32.

(50) Binder, W. H.; Sachsenhofer, R. *Macromol. Rapid Commun.* **2007**, *28*, 15.

(51) Binder, W. H.; Sachsenhofer, R. *Macromol. Rapid Commun.* **2008**, *29*, 952.

(52) Bock, V. D.; Hiemstra, H.; van Maarseveen, J. H. *Eur. J. Org. Chem.* **2006**, 51.

(53) Gallogly, M. M.; Starke, D. W.; Mieyal, J. J. *Antioxid. Redox Signaling* **2009**, *11*, 1059.

(54) Lukesh, J. C.; Palte, M. J.; Raines, R. T. *J. Am. Chem. Soc.* **2012**, *134*, 4057.

(55) Wiita, A. P.; Ainavarapu, R. K.; Huang, H. H.; Fernandez, J. M. *Proc. Natl. Acad. Sci. U. S. A.* **2006**, *103*, 7222.

(56) Singh, R.; Whitesides, G. M. *J. Am. Chem. Soc.* **1990**, *112*, 1190.